Original Paper — *Forma*, **9**, 51–66, 1994

Mathematical Modelling Consideration on AV-Node Action Potential Spectrum

Chie KOIDE and Hiromi SENO

Department of Mathematics, Faculty of Science, Hiroshima University, Kagamiyama 1-3-1, Higashi-Hiroshima 724, Japan

(Received August 17, 1993; Accepted April 15, 1994)

Keywords: $1/f^{\nu}$ Spectrum, AV-Node, Activation Pattern

Abstract. Two simple mathematical models for the electrical activation pattern of the AV-node action potential are considered. One is the model by Keener, and the other is its modification by the present authors. Spectral analyses of the activation patterns are carried out, and the power-laws in the range of high frequency are obtain. Some comparisons are mode with measured data.

1. Introduction

The heart is a complicated pump that circulates the blood through the body. It consists of specific muscles capable of spontaneous and rhythmical self-excitation. A pacemaker generates the proper periodic stimulus. Its periodicity is determined by integration of frequencies of cells forming the pacemaker. The resulting frequency is considered as possibly the best one that drives the heartbeat. The pacemaker is called *sinoatrial(SA)-node* (Fig. 1).

The SA-node is in the right atrial wall near the entrance of the superior vena cava, and the wave excited by it spreads throughout the right atrium. At the base of the atrium, the excitation wave encounters cells called *atrioventricular(AV)-node*, and then spreads to the left and the right ventricles via a specialized bundle of fibers, *His-Purkinje fibers* in the case of mammals. The AV-node brings the excitation wave from atrium to ventricle with a little delay due to its low conduction velocity. The muscle contraction of heart is caused by the depolarization of muscle membrane, caused by the spread of excitation wave. Therefore, the contraction of ventricle occurs later than that of atrium. This process leads to a high efficiency of blood-circulation work of heart.

Some simple mathematical models of such heartbeat cycle have been developed and analyzed (LEVINE, 1952; VASSALLE, 1966; NOBLE and TSIEN, 1968, 1969; LECAR and NOSSAL, 1971; FLAHERTY and HOPPENSTEADT, 1978; MILLER, 1979; GLASS *et al.*, 1980). KEENER (1981) modifies the mathematical model studied by LANDAHL and GRIFFEATH

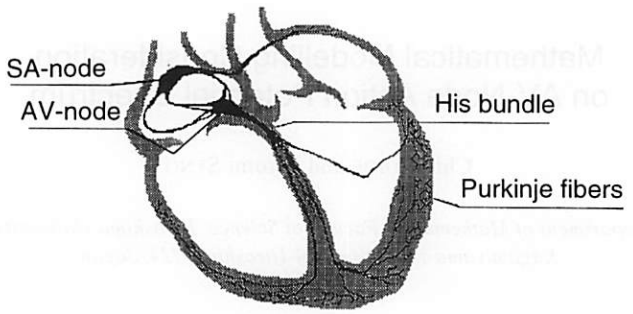

Fig. 1. The conduction system of mammal heart. Pulse from SA-node spreads to left and right ventricles through AV-node and His-Purkinje fibers. His-Purkinje fibers have fractal-like structure.

(1971), combining two dynamics for the electrical activation of the ventricles and its excitatory threshold. The model by KEENER (1981) can realize some of specific aperiodic heartbeat patterns, which are known as cardiac arrythmia. Generally, the arrythmia has some causes to drive abnormal rhythms. In KEENER's model (1981), AV Conduction Block is considered by using properties of circle maps for the model system, and it is shown that large period and aperiodic heartbeat patterns occur only in narrow parameter regions, and therefore are rarely observed in clinical situation.

On the other hand, GOLDBERGER *et al.* (1985) discuss the $1/f^{\nu}$ power-law for high frequency range in the heartbeat spectra ($\nu = 3.8 \sim 4.3$), based on a mathematical model for a conduction process through the fractal structure of His-Purkinje fibers (as for fractal concept, for instance, refer MANDELBROT, 1983). Although the spectral analyses of some sampled pattern of heartbeat of human and animals indicate the $1/f^{\nu}$ power-law in high frequency range (HOOGE *et al.*, 1981; KOBAYASHI and MUSHA, 1982; MONTROLL and SHLESINGER, 1982; GOLDBERGER, 1990; WEST, 1990; CHIALVO and JALIFE, 1991; LEWIS and GUEVARA, 1991), the argument by GOLDBERGER *et al.* (1985) seems not to explain well every $1/f^{\nu}$ power-laws, because their model is based on the fractal nature of conduction path, which is not always expected for the conduction system of some animals. LEWIS and GUEVARA (1991) showed that non-fractal conduction process can also lead the $1/f^{\nu}$ power-law by analyzing a simple triangular pulse ($\nu = 4.0$) and a one-dimensional cable model for the ionic currents ($\nu = 3.2$). In addition, CHIALVO and JALIFE (1991) showed the corresponding results by analyzing the data from a normal activated frog electrographic complex ($\nu = 2.02$) and a frog sciatic nerve ($\nu = 2.84$). Mathematical analysis of such power-law independent of fractal structure is still an open-problem.

In this paper, is presented a mathematical analysis of AV-node firing by two types of dynamical models: one studied by KEENER (1981) and the other modified by us. We especially analyze the spectra for AV-node action potential pattern, as GOLDBERGER *et al.* (1985) did for the electrocardiogram waveform. By our model analyses, it is found that the power-law nature might be expected also for AV-node potential spectrum.

2. Statement of Model

2.1. Modelling assumptions

We consider only the normal rhythmic firing of AV-node, excluding the arrythmia. This means that our analysis is restricted to some region of parameters of our model.

Our model is based on two basic ideas. First, when SA-node fires, the tissue surrounding AV-node receives an excitatory voltage impulse to increase its action potential. If the action potential becomes sufficiently high beyond a threshold, AV-node fires causing contraction of the ventricle. Second, whenever there are AV-node firing and ventricular contraction, the threshold of AV-node instantaneously increases and then gradually decreases, waiting for the next SA-node firing. The process of AV-node firing satisfies the following assumptions:

i) SA-node fires regularly with period $\hat{T}$.

ii) Influence of excitatory voltage impulse by SA-node firing causes increase of the AV-node action potential v.

iii) At the moment when the AV-node action potential v becomes equal to the threshold u for AV-node, that is, when $u = v$, AV-node fires.

iv) Whenever AV-node fires, the threshold u increases by a fixed increment Δu. After the increase, the threshold switches to decrease.

v) The subsequent SA-node firing promotes the increase of the AV-node action potential.

2.2. Model 1 (Keener's model)

The n-th SA-node firing produces a current pulse which reaches AV-node at $t = 0$. The pulse takes the following form at AV-node until the next pulse arrives from SA-node:

$$I(t) = I_0 e^{-\beta t} \quad \left(0 \leqslant t < \hat{T}\right), \tag{1}$$

where I_0 and β are positive constants. Equation (1) is defined during $0 \leqslant t < \hat{T}$, because the pulse produced by the next SA-node firing reaches AV-node at $t = \hat{T}$.

During $0 \leqslant t < \hat{T}$ after the arrival of the n-th pulse from SA-node, the AV-node action potential $v_n(t)$ is assumed to be governed by the following dynamics:

$$\frac{dv_n(t)}{dt} = KI_0 e^{-\beta t} - \alpha v_n(t) \quad \left(0 \leqslant t < \hat{T}\right), \tag{2}$$

$$v_n(0) = v_{n-1}\left(\hat{T}\right), \tag{3}$$

where K and α are positive constants. K indicates the effect of the current pulse from SA-

node. α corresponds to the decay rate of the AV-node potential. Equation (3) means the continuity of the AV-node potential.

The threshold for AV-node firing, $u_n(t)$, is governed by

$$\frac{du_n(t)}{dt} = -\gamma u_n(t) + \delta(t - \tau_n)\Delta u \quad \left(0 \leqslant t < \hat{T}\right), \tag{4}$$

$$u_n(0) = u_{n-1}\left(\hat{T}\right), \tag{5}$$

where Δu is the increment of threshold at the n-th AV-node firing time τ_n ($0 \leqslant \tau_n \leqslant \hat{T}$). $\delta(t)$ denotes the usual Dirac-delta function: $\delta(t) = +\infty$ for $t = 0$; $\delta(t) = 0$ otherwise. The firing time τ_n is given by the assumption (iii) as follows (see also Fig. 2):

$$v_n(\tau_n) = \lim_{t \uparrow \tau_n} u_n(t). \tag{6}$$

Note that $v_n(t)$ changes independent of the behaviour of $u_n(t)$ in Model 1.

In the next period of length $\hat{T}$ after the $n+1$-th pulse arrives at AV-node, $v_{n+1}(t)$, $u_{n+1}(t)$ and τ_{n+1} are defined in the same way.

2.3. *Model 2*

The potential $v_n(t)$ possibly receive some effect of AV-node firing, since the action potential could be influenced by the firing process. Therefore, it is meaningful to modify Model 1. One natural way of modification is given below as Model 2:

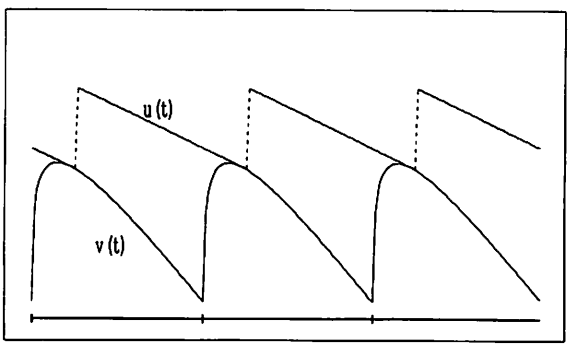

Fig. 2. The stationary oscillations $v_\infty(t)$ and $u_\infty(t)$ of Model 1, computed with parameters: $\alpha = 10.0$; $\beta = 9.0$; $\Delta u = 0.20$; $\hat{T} = 0.72$; $\tau_\infty = 0.18$. The ordinate axis has log-scale.

$$\frac{dv_n(t)}{dt} = \begin{cases} KI_0 e^{-\beta t} & \left(0 \leqslant t < \tau_n\right), \\ -\alpha v_n(t) & \left(\tau_n \leqslant t < \hat{T}\right), \end{cases} \tag{7}$$

$$v_n(0) = u_{n-1}\left(\hat{T}\right). \tag{8}$$

In this model, $v_n(t)$ increases until the AV-node firing ($t = \tau_n$), and after that, it decreases with the decay rate α. The threshold $u_n(t)$ is given the same as in Model 1.

3. Analysis

3.1. Model 1

The solution of Eqs. (2), (3), (4) and (5) is (for derivation, see Appendix A)

$$v_n(t) = \left[A\left\{ -B - \frac{\left(e^{-\beta\hat{T}} - e^{-\alpha\hat{T}}\right)e^{-(n-1)\alpha\hat{T}}}{1 - e^{-\alpha\hat{T}}} \right\} + v_0 e^{-(n-1)\alpha\hat{T}} \right] e^{-\alpha t} + Ae^{-\beta t}$$
$$\left(1 \leqslant n,\ 0 \leqslant t \leqslant \hat{T}\right), \tag{9}$$

$$v_1(0) = v_0 > 0, \tag{10}$$

$$u_n(t) = \begin{cases} \left(v_{n-1}\left(\tau_{n-1}\right) + \Delta u\right)e^{-\gamma\left(\hat{T} - \tau_{n-1} + t\right)} & \left(2 \leqslant n,\ 0 \leqslant t < \tau_n\right), \\ \left(v_n\left(\tau_n\right) + \Delta u\right)e^{-\gamma\left(t - \tau_n\right)} & \left(2 \leqslant n,\ \tau_n \leqslant t \leqslant \hat{T}\right), \end{cases} \tag{11}$$

$$u_1(t) = \begin{cases} u_0 e^{-\gamma t} & \left(0 \leqslant t < \tau_1\right), \\ \left(v_1\left(\tau_1\right) + \Delta u\right)e^{-\gamma\left(t - \tau_1\right)} & \left(\tau_1 \leqslant t \leqslant \hat{T}\right), \end{cases} \tag{12}$$

$$u_1(0) = u_0 > v_0, \tag{13}$$

where v_0 and u_0 are initial values of $v_1(t)$ and $u_1(t)$, and

$$A = \frac{KI_0}{\alpha - \beta}, \quad B = \frac{1 - e^{-\beta \hat{T}}}{1 - e^{-\alpha \hat{T}}}. \tag{14}$$

As mentioned before, we focus on the stationary regular behaviour, i.e. $(v_\infty(t), u_\infty(t))$. In other words, it is assumed that, for each n, τ_n is uniquely determined by (6) with the initial τ_1 calculated from (9) and (12), and then converges to a τ_∞ such that $0 \leqq \tau_\infty \leqq \hat{T}$. This assumption means a constraint on the parameters, as given analytically by KEENER (1981).

For $n \to \infty$, the periodic stationary state with period $\hat{T}$ is described as follows:

$$v_\infty(t) = A\left(-Be^{-\alpha t} + e^{-\beta t}\right) \quad \left(0 \leqq t \leqq \hat{T}\right), \tag{15}$$

$$u_\infty(t) = \begin{cases} \left(v_\infty(\tau_\infty) + \Delta u\right) e^{-\gamma\left(\hat{T} - \tau_\infty + t\right)} & \left(0 \leqq t < \tau_\infty\right), \\ \left(v_\infty(\tau_\infty) + \Delta u\right) e^{-\gamma(t - \tau_\infty)} & \left(\tau_\infty \leqq t \leqq \hat{T}\right). \end{cases} \tag{16}$$

Remark that $v_\infty(0) = v_\infty(\hat{T})$ in this stationary state. τ_∞ is determined as the root of the following equation on $[0, \hat{T}]$ (Appendix B):

$$-Be^{-\alpha \tau_\infty} + e^{-\beta \tau_\infty} = \frac{\Delta u}{A\left(e^{\gamma \hat{T}} - 1\right)}. \tag{17}$$

The uniqueness of τ_∞ requires the following conditions on parameters (Appendix B):

i) When $\alpha B/\beta \leqq 1$,

$$-Be^{-\alpha \hat{T}} + e^{-\beta \hat{T}} \leqq \frac{\Delta u}{A\left(e^{\gamma \hat{T}} - 1\right)} \leqq 1 - B; \tag{18}$$

ii) When $1 < \alpha B/\beta < e^{(\alpha - \beta)\hat{T}}$,

$$\min\left(1 - B, -Be^{-\alpha \hat{T}} + e^{-\beta \hat{T}}\right) \leqq \frac{\Delta u}{A\left(e^{\gamma \hat{T}} - 1\right)} \leqq B\left(\frac{\alpha}{\beta} - 1\right)\left(\frac{\alpha B}{\beta}\right)^{-\alpha/(\alpha - \beta)}; \tag{19}$$

iii) When $e^{(\alpha - \beta)\hat{T}} \leqq \alpha B/\beta$,

$$1-B \leqq \frac{\Delta u}{A\left(e^{\gamma \hat{T}}-1\right)} \leqq -Be^{-\alpha \hat{T}}+e^{-\beta \hat{T}}. \tag{20}$$

Note that, in the case when $1 < \alpha B/\beta < e^{(\alpha-\beta)\hat{T}}$, there can be two distinct roots of (17). Then, the smaller is chosen as τ_∞, because of the definition for AV-node firing moment (see the assumption (iii)). The above conditions are necessary for the regular behaviour (of $(v_\infty(t), u_\infty(t))$ (see KEENER, 1981). The stationary state $(v_\infty(t), u_\infty(t))$ is shown in Fig. 2 for $\alpha = 10.0$, $\beta = 9.0$, $\Delta u = 0.2$, $\hat{T} = 0.72$, and $\tau_\infty = 0.18$.

Since our interest is the spectrum of normal periodic behaviour of AV-node potential, we hereafter focus on the behaviour of $v_\infty(t)$. The Fourier transformation of $v_\infty(t)$ gives the following power-energy spectrum function $V(\omega)$:

$$\begin{aligned} V(\omega) &= \frac{1}{2\pi}\int_0^{\hat{T}} v_\infty(t)e^{-i\omega t}\mathrm{d}t \\ &= \frac{A}{2\pi}\left\{\left(\frac{B}{\alpha+i\omega}e^{-\alpha\hat{T}}-\frac{1}{\beta+i\omega}e^{-\beta\hat{T}}\right)e^{-i\omega\hat{T}}-\frac{B}{\alpha+i\omega}+\frac{1}{\beta+i\omega}\right\}. \end{aligned} \tag{21}$$

Now, we can derive the energy spectrum $S(\omega) \equiv |V(\omega)|^2$ as follows:

$$\begin{aligned} S(\omega) = \frac{A^2}{4\pi^2\left(\beta^2-\alpha^2\right)}\Bigg[&\left\{B^2\left(e^{-2\alpha\hat{T}}+1\right)-2B\left(e^{-(\alpha+\beta)\hat{T}}+1\right)+e^{-2\beta\hat{T}}+1\right. \\ &\left.+2(1-B)\cos\left(\omega\hat{T}\right)\left(Be^{-\alpha\hat{T}}-e^{-\beta\hat{T}}\right)\right\}\left(\frac{\omega^2}{\alpha^2+\omega^2}-\frac{\omega^2}{\beta^2+\omega^2}\right) \\ &+2B(\alpha-\beta)\sin\left(\omega\hat{T}\right)\left(e^{-\alpha\hat{T}}-e^{-\beta\hat{T}}\right)\left(\frac{\omega}{\alpha^2+\omega^2}-\frac{\omega}{\beta^2+\omega^2}\right) \\ &+\left\{B^2\left(e^{-2\alpha\hat{T}}+1-2e^{-\alpha\hat{T}}\cos\left(\omega\hat{T}\right)\right)\beta^2\right. \\ &-2B\left(e^{-(\alpha+\beta)\hat{T}}+1-\cos\left(\omega\hat{T}\right)\left(e^{-\alpha\hat{T}}+e^{-\beta\hat{T}}\right)\right)\alpha\beta \\ &\left.+\left(e^{-2\beta\hat{T}}+1-2e^{-\beta\hat{T}}\cos\left(\omega\hat{T}\right)\right)\alpha^2\right\}\left(\frac{1}{\alpha^2+\omega^2}-\frac{1}{\beta^2+\omega^2}\right)\Bigg]. \end{aligned} \tag{22}$$

After Taylor expansion in terms of $1/\omega$, we obtain

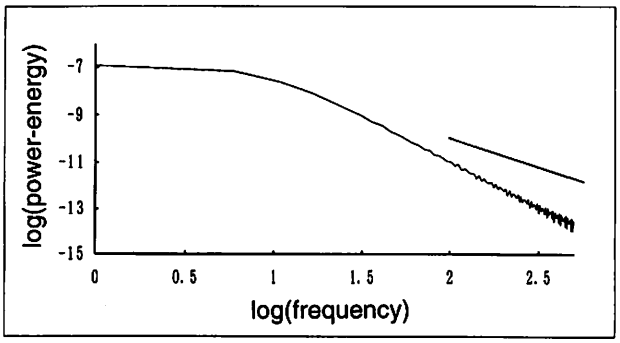

Fig. 3. Power spectrum of $v_\infty(t)$ shown in Fig. 2. In the high frequency range, $1/f^2$ power-law is observed.

$$S(\omega) \approx \frac{A^2}{4\pi^2}\left\{B^2\left(e^{-2\alpha\hat{T}}+1\right)-2B\left(e^{-(\alpha+\beta)\hat{T}}+1\right)+e^{-2\beta\hat{T}}+1 \right.$$
$$\left. +2(1-B)\cos\left(\omega\hat{T}\right)\left(Be^{-\alpha\hat{T}}-e^{-\beta\hat{T}}\right)\right\}\frac{1}{\omega^2}$$
$$+\frac{A^2}{2\pi^2}\left\{B(\alpha-\beta)\sin\left(\omega\hat{T}\right)\left(e^{-\alpha\hat{T}}-e^{-\beta\hat{T}}\right)\right\}\frac{1}{\omega^3}+O\left(\frac{1}{\omega^4}\right). \tag{23}$$

This result demonstrates the $1/f^2$ characteristics of AV-node action potential in the high frequency range. An exemplifying power-energy spectrum computed numerically is presented in Fig. 3 for $\alpha = 10.0$, $\beta = 9.0$, $\Delta u = 0.2$, $\hat{T} = 0.72$, and $\tau_\infty = 0.18$.

3.2. *Model 2*

The solution of Eqs. (7) and (8) is given by (see Appendix C)

$$v_n(t) = \begin{cases} v_0 e^{-\alpha\sum_{k=1}^{n-1}\left(\hat{T}-\tau_k\right)} + C\left(1-e^{-\beta t}\right) \\ \quad + C\sum_{k=1}^{n-1}\left(1-e^{-\beta\tau_k}\right)e^{-\alpha\sum_{i=k}^{n-1}\left(\hat{T}-\tau_i\right)} \quad \left(2\leqslant n,\ 0\leqslant t<\tau_n\right), \\ e^{-\alpha\left(t-\tau_n\right)}\left\{v_0 e^{-\alpha\sum_{k=1}^{n-1}\left(\hat{T}-\tau_k\right)} + C\left(1-e^{-\beta\tau_n}\right)\right. \\ \quad \left. + C\sum_{k=1}^{n-1}\left(1-e^{-\beta\tau_k}\right)e^{-\alpha\sum_{i=k}^{n-1}\left(\hat{T}-\tau_i\right)}\right\} \left(2\leqslant n,\ \tau_n\leqslant t\leqslant\hat{T}\right), \end{cases} \tag{24}$$

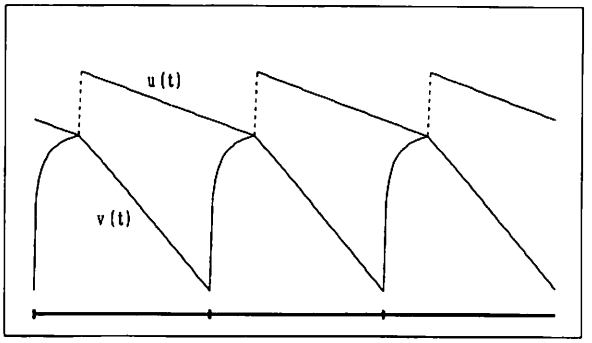

Fig. 4. The stationary oscillations $v_\infty(t)$ and $u_\infty(t)$ of Model 2, computed with parameters: $\alpha = 10.0$; $\beta = 9.0$; $\Delta u = 0.20$; $\hat{T} = 0.72$; $\tau_\infty = 0.18$. The ordinate axis has log-scale.

$$v_1(t) = \begin{cases} v_0 + C\left(1 - e^{-\beta t}\right) & \left(0 \leqslant t < \tau_1\right), \\ e^{-\alpha(t-\tau_1)}\left\{v_0 + C\left(1 - e^{-\beta\tau_1}\right)\right\} & \left(\tau_1 \leqslant t \leqslant \hat{T}\right), \end{cases} \tag{25}$$

$$v_1(0) = v_0 > 0, \tag{26}$$

where τ_n is assumed to be uniquely determined as in Model 1, and

$$C = \frac{\alpha - \beta}{\beta} A. \tag{27}$$

The periodic stationary state for $v_\infty(t)$ is (see Fig. 4 and Appendix D)

$$v_\infty(t) = \begin{cases} C\left(1 - e^{-\beta t}\right) + D\Delta u & \left(0 \leqslant t < \tau_\infty\right), \\ De^{-\alpha\left(t - \hat{T}\right)}\Delta u & \left(\tau_\infty \leqslant t \leqslant \hat{T}\right), \end{cases} \tag{28}$$

where

$$D = \frac{e^{-\alpha\left(\hat{T} - \tau_\infty\right)}}{e^{\gamma\hat{T}} - 1}, \tag{29}$$

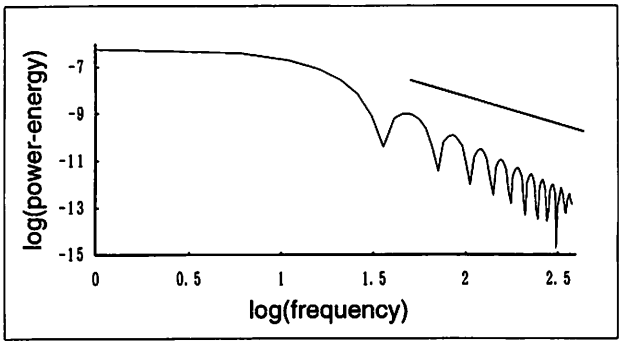

Fig. 5. Power spectrum $v_\infty(t)$ shown in Fig. 4. In the high frequency range, $1/f^2$ power-law is observed.

and τ_∞ is uniquely determined as the root for the following equation on $[0, \hat{T}]$ (Appendix E):

$$C\left(1-e^{-\beta\tau_\infty}\right)=D\left(e^{-\alpha\left(\tau_\infty-\hat{T}\right)}-1\right)\Delta u. \tag{30}$$

$u_\infty(t)$ is given by (17) with the above $v_\infty(t)$ and τ_∞.

The spectrum function $V(\omega)$ for the stationary behaviour of AV-node action potential is

$$\begin{aligned} V(\omega)=\frac{1}{2\pi}\Bigg[&\frac{1}{i\omega}(C+D\Delta u)\left(1-e^{-i\omega\tau_\infty}\right)\\ &+\frac{1}{\alpha+i\omega}e^{\alpha\hat{T}}D\Delta u\left(e^{-(\alpha+i\omega)\tau_\infty}-e^{-(\alpha+i\omega)\hat{T}}\right)\\ &+\frac{1}{\beta+i\omega}C\left(e^{-(\beta+i\omega)\tau_\infty}-1\right)\Bigg], \end{aligned} \tag{31}$$

and the energy spectrum $S(\omega)$ after Taylor expansion is obtained as

$$
\begin{aligned}
S(\omega) \approx \frac{1}{2\pi^2}\Big[&(C+D\Delta u)^2\left(1-\cos(\omega\tau_\infty)\right)\\
&+e^{2\alpha\hat{T}}(D\Delta u)^2\left\{\frac{e^{-2\alpha\tau_\infty}+e^{-2\alpha\hat{T}}}{2}-e^{-\alpha\left(\tau_\infty+\hat{T}\right)}\cos\left(\omega\left(\tau_\infty-\hat{T}\right)\right)\right.\\
&+\frac{C+D\Delta u}{\Delta u}e^{-\alpha\hat{T}}\left(-e^{-\alpha\tau_\infty}+e^{-\alpha\tau_\infty}\cos(\omega\tau_\infty)\right.\\
&\left.\left.-e^{-\alpha\hat{T}}\cos\left(\omega\hat{T}\right)+e^{-\alpha\hat{T}}\cos\left(\omega\left(\hat{T}-\tau_\infty\right)\right)\right)\right\}\\
&+C^2\left\{\frac{e^{-2\beta\tau_\infty}+1}{2}-e^{-\beta\tau_\infty}\cos(\omega\tau_\infty)\right.\\
&\left.+\frac{C+D\Delta u}{C}\left(e^{-\beta\tau_\infty}+1\right)\left(\cos(\omega\tau_\infty)-1\right)\right\}\\
&+e^{\alpha\hat{T}}CD\Delta u\left\{e^{-(\alpha+\beta)\tau_\infty}-e^{-\alpha\hat{T}-\beta\tau_\infty}\cos\left(\omega\left(\hat{T}-\tau_\infty\right)\right)\right.\\
&\left.-e^{-\alpha\tau_\infty}\cos(\omega\tau_\infty)+e^{-\alpha\hat{T}}\cos\left(\omega\hat{T}\right)\right\}\Big]\frac{1}{\omega^2}\\
+\frac{1}{2\pi^2}\Big[&\alpha e^{\alpha\hat{T}}D\Delta u(C+D\Delta u)\left\{e^{-\alpha\tau_\infty}\sin(\omega\tau_\infty)\right.\\
&\left.-e^{-\alpha\hat{T}}\sin\left(\omega\hat{T}\right)+e^{-\alpha\hat{T}}\sin\left(\omega\left(\hat{T}-\tau_\infty\right)\right)\right\}\\
&+(C+D\Delta u)C\beta\left(e^{-\beta\tau_\infty}-1\right)\sin(\omega\tau_\infty)\\
&-e^{\alpha\hat{T}}CD\Delta u(\alpha-\beta)\left\{e^{-\alpha\hat{T}-\beta\tau_\infty}\sin\left(\omega\left(\hat{T}-\tau_\infty\right)\right)\right.\\
&\left.+e^{-\alpha\tau_\infty}\sin(\omega\tau_\infty)-e^{-\alpha\hat{T}}\sin\left(\omega\hat{T}\right)\right\}\Big]\frac{1}{\omega^3}+O\left(\frac{1}{\omega^4}\right).
\end{aligned}
\tag{32}
$$

For sufficiently large ω, we obtain $1/f^2$ characteristics of AV-node action potential (see Fig. 5).

4. Discussion

In this paper, we have proposed a model which is modified from Keener's model by considering the influence of the threshold variation $u_n(t)$ on the AV-node action potential $v_n(t)$, and have given its exact solution. It can be shown that this solution yields also a $1/f^2$ spectrum as in Keener's model.

Our results indicate that non-fractal system for heartbeat can show the power-law characteristics in its power spectrum in the high frequency region. Although our object of modelling is not the electrocardiographic complex as in GOLDBERGER *et al.* (1985) and the others, but the temporal variation pattern of AV-node action potential, the comparison of the power-laws of AV-node action potential pattern with that of electrocardiographic complex may be possible. For example, $1/f^{\nu}$ power-law for large f does not necessarily depend on any fractal structure of heartbeat system, which would be applied also to the electrocardiographic complex.

It is worth nothing that both Model 1 and Model 2 yields $1/f^{\nu}$ power-law with $\nu = 2$ in the range of high frequency. On the other hand, a triangular pulse has $1/f^{\nu}$ power-law nature with $\nu = 4$ (LEWIS and GUEVARA, 1991), which is significantly different from our $\nu = 2$. This means that the shape of pulse causes $1/f^{\nu}$ power-law characteristics, and the index ν significantly depends on the intrinsic dynamics which drives the pulse.

Moreover, $1/f^{\nu}$ power-law characteristics sampled from human electrocardiographic complex give $\nu = 3.8$~4.3 (GOLDBERGER *et al.*, 1985), while $\nu = 2.02$ for a normal activated frog electrographic complex, and $\nu = 2.84$ for a frog sciatic nerve (CHIALVO and JALIFE, 1991). Our result $\nu = 2$ is too small for human electrocardiographic complex, and near to that for frog electrographic complex. Since, in our model, any structure of conduction network system is not introduced, our model might be comparable with such simple conduction systems as that of frog. In short, it is suggested that simple neural conduction systems would have $1/f^{\nu}$ power-law nature with $\nu \approx 2$, while more complex ones, such as that by GOLDBERGER *et al.* (1985), would have the nature with larger ν.

Although the model by GOLDBERGER *et al.* (1985), based on the fractal spatial structure of His-Purkinje fibers, cannot explain some other power-law characteristics in spatially non-fractal conduction system, there may be a possibility that a combination of spatial and temporal fractal structure of conduction dynamics leads to $1/f^{\nu}$ power-law nature of relatively complex conduction system. Mathematical modelling by networking oscillator coupled with our model, for example, seems to be another possible way to give some valuable aspects on such conduction system. It should be noted also that we need to consider low frequency fluctuations for a better discussion of fractality.

There are other complicated models of neuronal firing such as the FitzHugh-Nagumo model (FITZHUGH, 1961; MCKEAN, 1970) or Hodgkin-Huxley model (HODGKIN and HUXLEY, 1952) based on the ionic currents across an excitable. However, simplified models can be treated regorously, and can still reflect physiological reality. Response of more complicated models to periodic inputs is far from complete understanding and still open-problem (FLAHERTY and HOPPENSTEADT, 1978).

The authors are grateful to Prof. Ryuji Takaki and anonymous referee for their helpful comments to complete this paper.

APPENDIX A

From Eqs. (2) and (3), we have

$$v_n(t) = v_{n-1}\left(\hat{T}\right)e^{-\alpha t} + A\left(e^{-\beta t} - e^{-\alpha t}\right), \tag{A1}$$

where A is given by (14). At $t = T$, this solution becomes

$$v_1\left(\hat{T}\right) = v_0 e^{-\alpha \hat{T}} + A\left(e^{-\beta \hat{T}} - e^{-\alpha \hat{T}}\right), \tag{A2}$$

$$v_n\left(\hat{T}\right) = v_{n-1}\left(\hat{T}\right)e^{-\alpha \hat{T}} + A\left(e^{-\beta \hat{T}} - e^{-\alpha \hat{T}}\right). \tag{A3}$$

Solving (A3) with (A2), we arrive at

$$v_n\left(\hat{T}\right) = A\left(e^{-\beta \hat{T}} - e^{-\alpha \hat{T}}\right)\left\{\frac{1 - e^{-n\alpha \hat{T}}}{1 - e^{-\alpha \hat{T}}}\right\} + v_0 e^{-n\alpha \hat{T}}. \tag{A4}$$

Then, substituting (A4) into (A1), we get (9).

APPENDIX B

Since τ_∞ must satisfy Eq. (6), the following equation must be satisfied:

$$\left(v_\infty(\tau_\infty) + \Delta u\right)e^{-\gamma \hat{T}} = v_\infty(\tau_\infty). \tag{B1}$$

Substituting (15) into (B1), we obtain (17).

Now, we consider the following positive constant E and function $F(\tau)$:

$$E = \frac{\Delta u}{A\left(e^{\gamma \hat{T}} - 1\right)} > 0,$$

$$F(\tau) = -Be^{-\alpha \tau} + e^{-\beta \tau} \quad \left(0 \leqslant \tau \leqslant \hat{T}\right).$$

Then, from (17), τ_∞ is given by the root of $F(\tau) = E$. Here, $F(\tau)$ is smooth (C^1-class) on $[0, \hat{T}]$. The first derivative of $F(\tau)$ can be calculated as follows:

$$F'(\tau) = \alpha Be^{-\alpha \tau} - \beta e^{-\beta \tau}. \tag{B2}$$

The value of τ_* satisfying $F'(\tau_*) = 0$ is

$$\tau_* = \frac{1}{\alpha - \beta} \log \frac{\alpha B}{\beta}.$$

From (B2), the following statements on τ_∞ are obtained:

i) $\tau_* \leqq 0$, when $\alpha B/\beta \leqq 1$. Then, $F(\tau)$ is monotonically decreasing on $[0, \hat{T}]$. Therefore, only when $F(\hat{T}) \leqq E \leqq F(0)$, τ_∞ can be uniquely determined.

ii) $0 < \tau_* < \hat{T}$, when $1 < \alpha B/\beta < e^{(\alpha-\beta)\hat{T}}$. Then, $F(\tau)$ is unimodal. Therefore, only when $\min(F(0), F(\hat{T})) \leqq E \leqq F(\tau_*)$, τ_∞ can be determined. In the case when $\max(F(0), F(\hat{T})) \leqq E < F(\tau_*)$, two different roots for $F(\tau) = E$ can be obtained on $[0, \hat{T}]$. The smaller is chosen as τ_∞.

iii) $\hat{T} \leqq \tau_*$, when $e^{(\alpha-\beta)\hat{T}} \leqq \alpha B/\beta$. Then, $F(\tau)$ is monotonically increasing on $[0, \hat{T}]$. Therefore, only when $F(0) \leqq E \leqq F(\hat{T})$, τ_∞ can be uniquely determined.

These arguments lead to (18), (19) and (20).

APPENDIX C

From (7) and (8), the following solution is obtained:

$$v_n(t) = \begin{cases} v_{n-1}(\hat{T}) + C(1 - e^{-\beta t}) & (0 \leqq t < \tau_n), \\ e^{-\alpha(t-\tau_n)} \lim_{t \uparrow \tau_n} v_n(t) & (\tau_n \leqq t \leqq \hat{T}), \end{cases} \tag{C1}$$

where C is given by (27), hence, we obtain

$$v_1(\hat{T}) = e^{-\alpha(\hat{T}-\tau_1)}\left(v_0 + C\left(1 - e^{-\beta\tau_1}\right)\right), \tag{C2}$$

$$v_n(\hat{T}) = e^{-\alpha(\hat{T}-\tau_n)}\left(v_{n-1}(\hat{T}) + C\left(1 - e^{-\beta\tau_n}\right)\right). \tag{C3}$$

Solving (C3) with (C2), we can arrive at

$$v_n(\hat{T}) = v_0 e^{-\alpha\sum_{k=1}^{n}(\hat{T}-\tau_k)} + C\sum_{k=1}^{n}\left(1 - e^{-\beta\tau_k}\right)e^{-\alpha\sum_{i=k}^{n}(\hat{T}-\tau_i)}. \tag{C4}$$

Then, substituting (C4) into (C1), we get (24) and (25).

APPENDIX D

From Eqs. (6), (11) and (24), we have

$$v_{n+1}(\tau_{n+1}) = \left(v_n(\tau_n) + \Delta u\right) e^{-\gamma\left(\hat{T} - \tau_n + \tau_{n+1}\right)}.$$

For the stationary state, i.e. $n \to \infty$, we obtain

$$v_\infty(\tau_\infty) = \left(v_\infty(\tau_\infty) + \Delta u\right) e^{-\gamma \hat{T}},$$

hence,

$$v_\infty(\tau_\infty) = \frac{\Delta u}{e^{\gamma \hat{T}} - 1}. \tag{D1}$$

On the other hand, when $n \to \infty$ in (24), we have

$$v_\infty(t) = \begin{cases} \dfrac{KI_0}{\beta}\left(1 - e^{-\beta t}\right) + v_\infty(\tau_\infty) e^{\alpha\left(\tau_\infty - \hat{T}\right)} & \left(0 \leqq t < \tau_\infty\right), \\ v_\infty(\tau_\infty) e^{\alpha\left(\tau_\infty - t\right)} & \left(\tau_\infty \leqq t \leqq \hat{T}\right). \end{cases} \tag{D2}$$

Then, substituting (D1) into (D2), we get (27).

APPENDIX E

The quantity $v_\infty(\tau_\infty)$ is obtained by putting $t = \tau_\infty$ in (27), which yields (29). Now, we consider the following functions $G(\tau)$ and $H(\tau)$ on $[0, \hat{T}]$:

$$G(\tau) = C\left(1 - e^{-\beta \tau}\right),$$

$$H(\tau) = D\left(e^{-\alpha\left(\tau_\infty - \hat{T}\right)} - 1\right)\Delta u.$$

Then, τ_∞ is given by the root of $G(\tau) = H(\tau)$. Functions $G(\tau)$ and $H(\tau)$ are smooth (C^1-class) on $[0, \hat{T}]$. $G(\tau)$ is monotonically increasing on $[0, \hat{T}]$, while $H(\tau)$ is monotonically decreasing on $[0, \hat{T}]$. In addition it can be easily shown that $G(0) = 0 < H(0)$ and $H(\hat{T}) = 0 < G(\hat{T})$. Therefore, τ_∞ can be always uniquely determined.

REFERENCES

CHIALVO, D. R. and JALIFE, J. (1991) $1/f^{\alpha}$ power spectal density of the cardiac QRS complex is not associated with a fractal Purkinje system, *Biophys. J.*, **60**, 1303–1305.

FITZHUGH, R. (1961) Impulses and physiological states in models of nerve membrane, *Biophys. J.*, **1**, 445–466.

FLAHERTY, J. and HOPPENSTEADT, F. (1978) Frequency entrainment of a forced van der Pol oscillator, *Studies Appl. Math.*, **58**, 5–15.

GLASS, L., GRAVES, C., PETRILLO, G. A. and MACKEY, M. D. (1980) Unstable dynamics of a periodically driven oscillator in the presence of noise, *J. Theor. Biol.*, **86**, 455–476.

GOLDBERGER, A. L. (1990) Fractal electrodynamics of the heartbeat in mathematical approaches to cardiac arrythmias, *Ann. NY Acad. Sci.*, **591**, 402–409.

GOLDBERGER, A. L., BHARGAVA, V., WEST, B. J. and MANDELL, A. J. (1985) On a mechanism of cardiac electrical stability: the fractal hypothesis, *Biophys. J.*, **48**, 525–528.

HODGKIN, A. L. and HUXLEY, A. F. (1952) A quantitative description of membrane current and its application to conduction and excitation in nerve, *J. Physiol.*, **117**, 500.

HOOGE, F. N., KLEINPENNING, T. G. M. and VANDAMME, L. K. J. (1981) Experimental studies on $1/f^{\alpha}$ noise, *Rep. Prog. Phys.*, **44**, 479–532.

KEENER, J. P. (1981) On cardiac arrythmias: AV conduction block, *J. Math. Biology*, **12**, 215–225.

KOBAYASHI, M. and MUSHA, T. (1982) $1/f^{\alpha}$ fluctuation of heartbeat period, *IEEE Trans. Biomed. Eng.*, **29**, 456–457.

LANDAHL, H. D. and GRIFFEATH, D. (1971) A mathematical model for first degree block and the Wenckebach phenomenon, *Bull. Math. Biophys.*, **33**, 27–38.

LECAR, H. and NOSSAL, R. (1971) Theory of threshold fluctuations in nerves. I. Relationship between electrical noise and fluctuations in axson firing, *Biophys. J.*, **11**, 1048–1067.

LEVINE, S. A. (1952) *Clinical Heart Disease*, 4th ed., W. B. Saunders and Co., Philadelphia.

LEWIS, T. J. and GUEVARA, M. R. (1991) $1/f^{\alpha}$ power spectrum of the QRS complex does not imply fractal activation of the ventricles, *Biophys. J.*, **60**, 1297–1300.

MANDELBROT, B. B. (1983) *The Fractal Geometry of Nature*, W. H. Freeman Publishers, San Francisco.

MCKEAN, H. P. (1970) Nagumo's equation, *Adv. Math.*, **4**, 209–223.

MILLER, R. N. (1979) A simple model of delay, block and one way conduction in Purkinje fibers, *J. Math. Biol.*, **7**, 385–398.

MONTROLL, E. W. and SHLESINGER, M. F. (1982) On $1/f^{\alpha}$ noise and other distributions with long tails, *Proc. Natl. Acad. Sci. USA*, **79**, 3380–3383.

NOBLE, D. and TSIEN, R. W. (1968) The kinetics and rectifier properties of the slow potassium current in cardiac Purkinje fibers, *J. Physiol.*, **195**, 185–214.

NOBLE, D. and TSIEN, R. W. (1969) Outward membrane currents activated in the plateau range of potentials in cardiac Purkinje fibers, *J. Physiol.*, **200**, 205–231.

VASSALLE, M. (1966) An analysis of cardiac pacemaker potential by means of voltage clamp technique, *Am. J. Physiol.*, **210**, 1335–1341.

WEST, B. J. (1990) *Fractal Physiology and Chaos in Medicine*, World Scientific publishing Co., Singapore.